

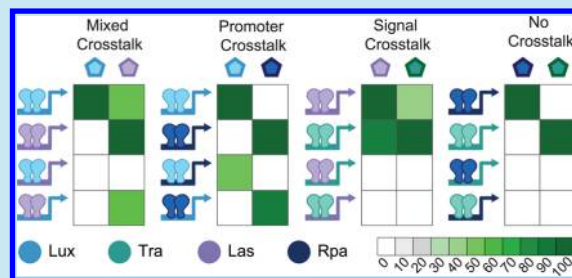
Quorum Sensing Communication Modules for Microbial Consortia

Spencer R. Scott[†] and Jeff Hasty^{*,†,‡,¶,||}[†]Department of Bioengineering, [‡]Molecular Biology Section, Division of Biological Science, and [¶]BioCircuits Institute, University of California, San Diego, La Jolla, California 92093, United States

S Supporting Information

ABSTRACT: The power of a single engineered organism is limited by its capacity for genetic modification. To circumvent the constraints of any singular microbe, a new frontier in synthetic biology is emerging: synthetic ecology, or the engineering of microbial consortia. Here we develop communication systems for such consortia in an effort to allow for complex social behavior across different members of a community. We posit that such communities will outpace monocultures in their ability to perform complicated tasks if communication among and between members of the community is well regulated. Quorum sensing was identified as the most promising candidate for precise control of engineered microbial ecosystems, due to its large diversity and established utility in synthetic biology. Through promoter and protein modification, we engineered two quorum sensing systems (rpa and tra) to add to the extensively used lux and las systems. By testing the cross-talk between all systems, we thoroughly characterized many new inducible systems for versatile control of engineered communities. Furthermore, we've identified several system pairs that exhibit useful types of orthogonality. Most notably, the tra and rpa systems were shown to have neither signal crosstalk nor promoter crosstalk for each other, making them completely orthogonal in operation. Overall, by characterizing the interactions between all four systems and their components, these circuits should lend themselves to higher-level genetic circuitry for use in microbial consortia.

KEYWORDS: synthetic ecology, quorum sensing, orthogonal, crosstalk, microbial consortia



Monoclonal synthetic biology has led to increased efficiency in the production of important industrial chemicals and “high value” products.^{1–3} However, the production capacity of a single organism is limited by metabolic load and byproduct toxicity, which are both difficult to address with intracellular genetic optimization.^{4–7} Furthermore, the defining goal of an engineered “superbug” capable of high-yield production⁸ is discordant with established ecological theory that the optimization of one trait occurs at the price of other necessary traits.^{9,10} Because of recent evidence that robust communities will out-perform optimized monocultures,¹¹ a new frontier in synthetic biology is emerging: synthetic ecology, or the engineering of microbial consortia.^{12–16}

Engineered microbial communities have already demonstrated that the limitations imposed by metabolic load can be addressed through distribution and specialization across various members of a community.^{17,18} This allows consortia to produce higher yields^{19,20} and to optimally respond to diauxic growth²¹ or harsh environmental fluctuations.^{22–24} Importantly, the engineering of microbial consortia will also facilitate a systematic understanding of native communities that are of increasing importance in the context of the human microbiome and significant environmental challenges.^{25–27}

Regulatory processes are essential for cooperative behavior in microbial consortia. Quorum sensing (QS) is a common mechanism used by bacteria to sense local cell density in order to coordinate gene expression and affect differential behavior.²⁸ Species capable of such sensing harbor regulator proteins that,

when bound to a particular ligand, modulate transcription from various QS promoters.²⁸ Although there are several different QS mechanisms,²⁹ the LuxR/LuxI-type systems mediated by homoserine lactone (HSL) ligands are the most promising due to their simplicity and large natural diversity.^{28,30,31} QS is a reliable and well-characterized tool synthetic biologists have used for a variety of applications including triggering biofilm formation,^{32,33} constructing synchronized oscillators,^{34,35} generating patterns,^{36,37} sensing pathogens,³⁸ and developing synthetic ecosystems.^{26,39} Furthermore, QS has proved to be a powerful tool for metabolic engineering, by allowing timed production of chemicals to commence at optimal cell-densities.^{40–43}

Taken collectively, these studies have established a foundation for the use of quorum sensing in microbial consortia. However, until recently,⁴⁴ the cross-interactions between QS systems have received little attention. If multiple systems are to be used in the same environment, it is important to know how they will interact with one another. Two QS systems in the same population can harbor either signal crosstalk, promoter crosstalk, or a mixture of both (Figure 1). Signal crosstalk occurs when a receptor can bind a non-canonical HSL, such as LuxR binding 3-oxo-C12-HSL (3OC12) which is native to the las system. Promoter crosstalk occurs when an activated receptor can bind a noncanonical

Received: December 16, 2015

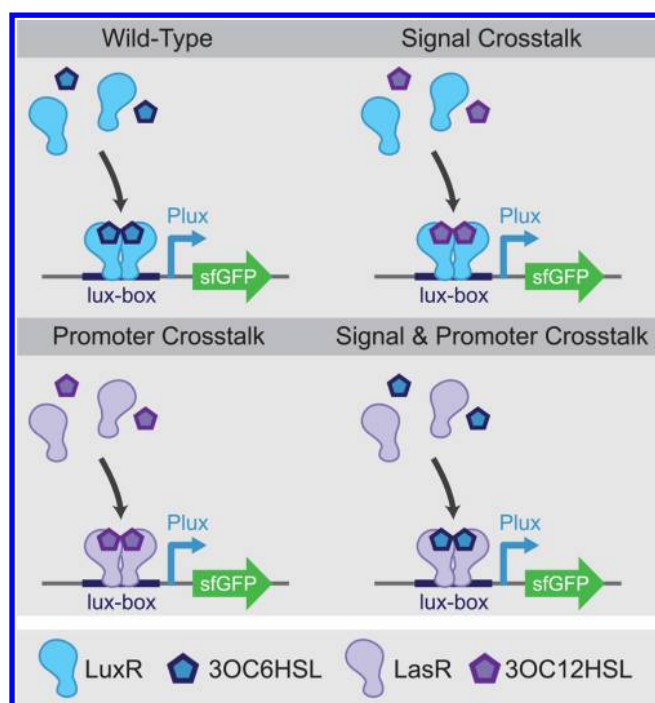


Figure 1. Potential sources of crosstalk between quorum sensing systems. Top left: R-protein (LuxR) binds its cognate ligand (3OC6HSL) to become active and drive transcription from the Plux promoter. Top right: Signal crosstalk occurs when the R-protein can become active through binding of an HSL other than its cognate ligand, such as LuxR binding 3OC12HSL, common to the las system. Bottom left: Promoter crosstalk occurs when the QS promoter of one system can be activated by the active R-protein of another system, such as Plux being activated by LasR bound to 3OC12HSL. Bottom right: Mixtures of both signal and promoter crosstalk can occur, allowing an R-protein from one system to bind an off-target ligand and activate a noncanonical promoter.

promoter, demonstrated by an activated LasR being capable of driving transcription off the Plux promoter. Covering all possible combinations reveals that a mixture of these two crosstalks is possible, whereby a receptor is activated by a noncanonical HSL and then activates a noncanonical promoter (Figure 1).

Through promoter and protein engineering, the rpa and tra quorum sensing systems were modified to allow functionality in *E. coli*, adding two more systems to the previously characterized lux and las systems. To the best of our knowledge the rpa system has never been described in *E. coli* before, and the tra system, although well-characterized in *A. tumefaciens* and *in vitro*,^{45–47} has otherwise been previously shown to exhibit poor activity in whole *E. coli* cells.⁴⁵ All possible cross-interactions between these systems' components were then tested to understand how they could be used in an engineered community.

Most systems exhibited varying levels of crosstalk, and while unexpected interference between components can cause a loss of circuit function,^{44,48} if the parts are well-characterized the crosstalk can be harnessed to create unique dynamical circuits. In other cases it can be advantageous to have communication systems that function orthogonally. For the purposes of this study, we defined orthogonality as such: system A is said to be “signal orthogonal” to system B if Receptor A cannot be activated by Signal B, “promoter orthogonal” to system B if Promoter A cannot be activated by an HSL-bound Receptor B,

and “completely orthogonal” if both cases are true. Orthogonality can therefore only be defined under a given concentration range of the signal and also depends on the definition of “activated”. We considered a system activated if it exhibited a maximum fold-change greater than 2, or an area under the curve (AUC) greater than 2% of the canonical AUC response, as defined for Figure 4.

Several groups have pointed out the utility of complete orthogonality⁴⁹ and even used different classes of QS systems^{50–52} in concert with Lux-like QS systems to accomplish such orthogonality. Here we demonstrate that different combinations of our Lux-like QS systems can achieve signal, promoter, and complete orthogonality. By characterizing the varying degrees of cross-talk and orthogonality between all four systems and their components, we hope to facilitate the development of synthetic microbial communities with well-controlled functionality.

2. RESULTS AND DISCUSSION

2.1. Screening Lux-like QS Systems.

Lux-like quorum sensing systems are widely dispersed throughout the proteobacteria phyla, each with a unique LuxR-like receptor and HSL homologue.^{29,53} Taking advantage of the natural diversity of these receptors and ligands, several systems were chosen based on their “evolutionary distance” and ligand uniqueness^{53,54} (see Supporting Information, Figure S1). The systems that were chosen include the lux system from *Vibrio fischeri* with ligand 3-oxo-C6-HSL (3OC6),⁵³ the las and rhl system from *Pseudomonas aeruginosa* with ligand 3OC12 and C4-HSL, respectively,⁵⁴ the tra system from *Agrobacterium tumefaciens* with ligand 3-oxo-C8-HSL (3OC8),⁴⁷ the rpa system from *Rhodospseudomonas palustris* with ligand p-coumaroyl-HSL (pC),^{55,56} the ahy system from *Aeromonas hydrophila*,⁵⁷ the sma system from *Serratia marcescens*,⁵⁸ the cer system from *Rhodobacter sphaeroides*,⁵⁹ and the exp system from *Sinorhizobium meliloti*.⁶⁰

To ensure reliable gene expression, each LuxR-like protein from the selected systems was GFP tagged to gauge translational output. After all of the R-protein-fusions were shown to express well (Figure 2A), each R-protein was tested for native functionality by cotransforming it with a GFP reporter plasmid harboring its native promoter (see Table S2^{46,56,59–63}). Despite evidence of successful expression of R-proteins, none of the systems other than the extensively characterized lux and las systems showed GFP induction in the presence of its HSL ligand. Several possible points of failure were identified; for example, protein misfolding may impede proper ligand or DNA binding, or recruitment of *E. coli*'s sigma factor may necessitate a slightly different protein location/conformation than the system's native chassis. To address these issues, we rationally designed and tested new promoters and proteins.

2.2. Rational Design of QS Systems.

Using the lux-system as a point of reference for a QS system that functions in *E. coli*, hybrid promoters Ptr* and Prpa* were created by replacing the lux-box in the commonly used PluxI promoter with the tra-box⁴⁷ and rpa-box,⁵⁶ respectively. This drastically improved the fold change of the rpa system from no-significant induction to nearly a 25× fold change in the presence of its cognate ligand (Figure 2B). The tra system was also improved from no significant induction, but its fold change was still rather low (Figure 2C). Observing protein alignment across several LuxR-homologues, it was noted TraR was missing a conserved

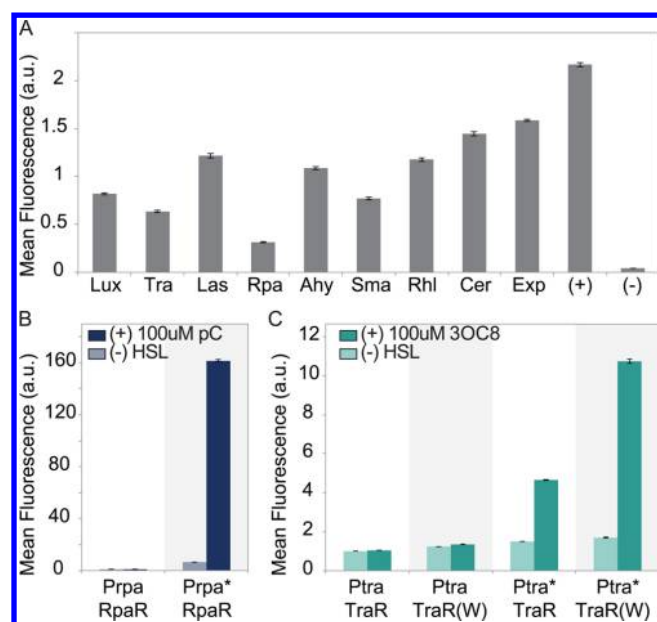


Figure 2. Engineering new QS systems in *E. coli* (A) Mean fluorescence of GFP-LuxR-like protein fusions. Positive control is constitutively expressed GFP, and negative control is the *E. coli* strain with no GFP plasmid. (B) Wild-type rpa-promoter is nonfunctional in *E. coli*, however an engineered Plux-rpa promoter functions well. (C) Wild type tra-promoter is also nonfunctional, but an engineered Plux-tra promoter shows significant fold-change in the presence of cognate ligand. Also, an engineered TraR with a point mutation to increase sigma factor binding increases fold change of the tra system. (B), (C) Mean values are normalized by lowest expression in each panel. Error bars represent SEM ($n = 3$).

tryptophan amino acid,⁶⁴ which in LuxR is known to be important for sigma factor recruitment.⁶⁵ Engineered receptor TraR(W) was created by substituting a tryptophan into the correct amino acid position. When combined with the Ptr* promoter and the native signal, the fold change was doubled compared to the wild-type TraR protein and hybrid Ptr* promoter (Figure 2C).

2.3. Quorum Sensing Circuit Multiplexing. To fully characterize the utility of these QS-responsive strains, a modular two-plasmid system was constructed such that an actuator plasmid constitutively produced the LuxR-like protein, while a reporter plasmid harbored a single QS-promoter expressing sfGFP (Figure 3A). With the four functional systems (lux, tra, las, and rpa), all 16 possible actuator/reporter two-plasmid strains were created. Each receptor protein, without any HSL ligand, has an inherent affinity for each promoter, giving each of these 16 combinations a unique basal expression level or “leakiness” (Table S1), defined as the GFP expression in the absence of any HSL ligand, normalized by the observed fluorescence of the same *E. coli* strain without a GFP plasmid (Figure S2). Leakiness can negatively affect genetic circuit functionality, or it can be harnessed to direct the rates of transient protein expression, making basal expression an important characteristic. Interestingly, the canonical R-protein and its respective promoter were seen to always harbor the highest leakiness for each promoter/receptor set. This finding suggests that if leakiness is an undesirable trait for a potential genetic circuit, a noncanonical yet functional R-protein could be used instead.

Each of these 16 strains were exogenously subjected to a wide concentration range of the four characteristic HSLs, and the resulting GFP production after 3 h of incubation was measured (Figure 3B). The concentration maximum (100 μ M) was limited by physiologically relevant numbers,³⁰ while the minimum (1×10^{-10} or 1×10^{-14} M) by previously observed response thresholds (data not shown). Only promoter/receptor pairs that showed a 2-fold induction or more in the presence of at least one HSL were shown in Figure 3, for all combinations not shown it can be inferred they exhibited no significant response under any conditions (Full data available, Figure S3 and Supplementary Data 1). QS constructs are denoted by a three letter system where “L” refers to the lux system, “T” to the tra system, “A” to the las system, and “R” to the rpa system; the first letter denotes the promoter used, the second letter denotes the R-protein used, and the third letter denotes the HSL used (Plux+LasR+3OC8= “LRT”). This fully comprehensive assay elucidated all three potential crosstalk dynamics, as well as extensively characterized many new inducible genetic circuits. Each construct’s relevant behavior was quantified by fitting its expression data to the typical dose–response function:

$$\text{GFP} = b + \frac{a - b}{1 + 10^{\log(\text{EC}_{50} - X)^*h}}$$

where a is the maximum response, b is the basal expression, X is the concentration of ligand, and GFP is the response at that concentration. To ensure meaningful fitted dose–response curves, only the QS pairs that showed significant activation before 100 μ M were analyzed. From this equation, four important attributes of each dose response curve were calculated: fold change, EC50, hill slope (h), and area under curve (AUC) or “activity area”^{66,67} (Table S1). Fold change is defined as the maximum observed expression divided by the basal expression in the absence of ligand (a/b). The EC50 is defined as the concentration of ligand that results in half-maximum activation of the QS construct. The hill slope is defined as the steepest slope along the dose response curve, and is indicative of how responsive the promoter/receptor pair is to the ligand. Lastly, the fitted curve was integrated using a trapezoidal function to calculate the area under the curve minus the area of the leakiness to give the activity area (Figure 4C). Generally, the Las system demonstrates the highest fold change and has a relatively low (strong) EC50, the Tra system has the lowest fold change and weakest EC50 but is also the least leaky. The Rpa system has the strongest EC50 and the highest leakiness, and the Lux system has midrange values for all characteristics.

Fold change is a very important aspect of genetic circuits, and this multiplex assay allowed the identification of systems with a wide range of induction curves ranging from 2-fold to almost 100-fold in batch culture after 3 h of induction (Figure 4A). However, the use of fold change as a standard to compare QS circuit performance was obfuscated by unexpected expression dynamics. For example, TTA shows a greater fold change than the canonical TTT, yet is much less sensitive to the exogenous ligand with an EC50 almost 2 orders of magnitude higher (Figure 4C). This phenomena may be the result of different HSL stabilities, but is more likely due to the receptor having a slightly different conformation when bound to the off-target HSL, allowing it to bind tighter to the DNA or recruit the sigma factor more strongly. Such a unique crosstalk dynamic may have implications in natural systems that would benefit

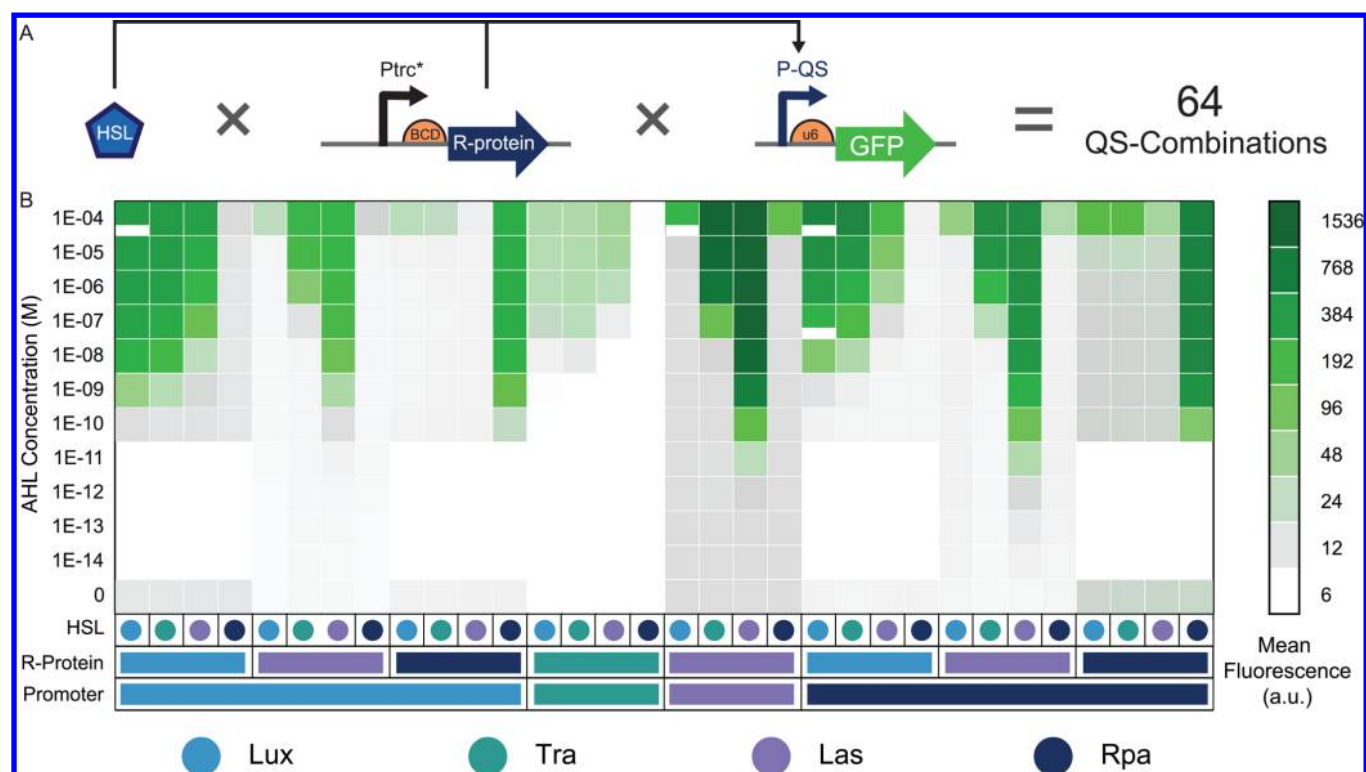


Figure 3. Dose–response from multiplexed quorum sensing circuits: (A) Genetic schematic of a single construct in the presence of a particular HSL ligand. With four R-proteins and four promoters there are 16 two-plasmid combinations each induced with four different HSLs giving 64 promoter/R-protein/HSL combinations measured at 8 ligand concentrations (or 12 for LasR). (B) Heat map showing GFP abundance for all QS combinations and HSL concentrations. Each column denotes a unique combination of signal (HSL), receptor (R-protein), and reporter (QS promoter), with rows denoting the concentration of ligand. Only Promoter/R-protein combinations that resulted in at least a 2-fold increase for one or more HSL are shown (full data *via* Figure S3 and Supplementary Data 1). Each value corresponds to the mean fluorescence value measured from a cell population normalized by the population's cell-density; all combinations and concentrations were done in triplicate.

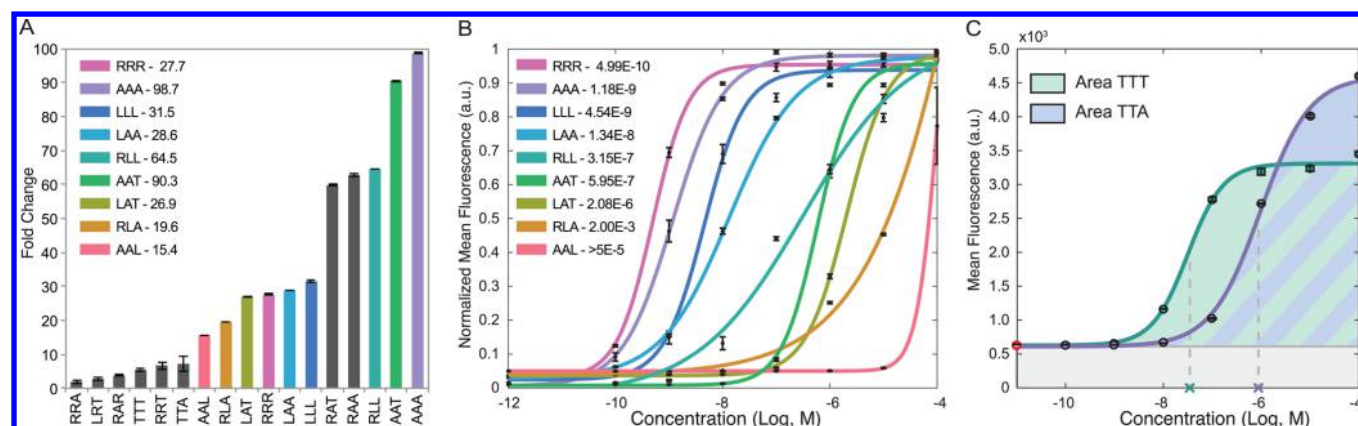


Figure 4. Activity area of dose–response curve as performance standard. (A) The maximum fold-change of a diverse subset of the QS constructs after 3 h of induction. (B) Normalized dose–response curves of a subset of QS constructs that demonstrate a variety of EC₅₀s. Each curve is normalized by its own maximum value, such that each curve converges to 1. (C) Fitted dose–response curves to the experimental data and their calculated activity areas. The red dot indicates the mean expression in the absence of HSL. Gray box under the curve represents the inherent leakiness of the circuit. Where the dotted lines meet the *x*-axis gives the EC₅₀ value. Error bars indicate the standard error of the mean ($n = 3$).

from a strong response to high levels of a foreign species. Fold change was further determined to be misleading because many systems showed steep increases in induction at 100 μ M, while at 10 μ M they still exhibited near-background expression (Figure S4). AAL, for instance, has a fold change of 15, yet its activity area is about 1% that of the canonical (AAA). The normalized activity area of 1% gives a much more accurate

account of its relative performance than the normalized fold change (15% of the max fold change) (Figure 4B).

Selection of constructs based on EC₅₀ could help create circuits with specific expression dynamics such as sequentially firing promoters based on cell density (Figure 4B). Additionally, systems in which the R-protein is completely orthogonal to a ligand until 100 μ M—since that concentration would be difficult to reach without exogenously provided signal—could

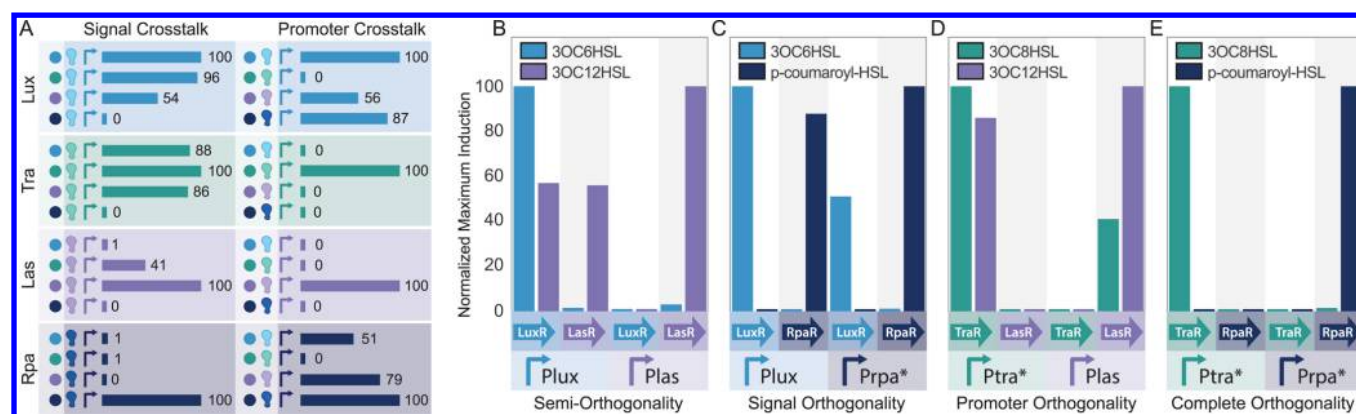


Figure 5. Identifying crosstalk and orthogonality between QS circuits. (A) Activity area of the fitted curve, across all HSL concentration values, is used to graphically represent every R-protein's affinity for each HSL ligand and each QS-promoter's ability to be activated by an off-target receptor. Left column: Signal crosstalk as demonstrated by each canonical promoter/R-protein pair's ability to be activated by nonspecific ligands. In each box, values are normalized by the maximum performance of that R-protein/Promoter pair (e.g., LLL/LLL = 96%). Right column: Activation of each promoter by each canonical R-protein/ligand pair, representing promoter crosstalk. In each box, values are normalized by the maximum performance of that promoter (e.g., LRR/LLL = 87%). (B–E) Comparisons of two sets of QS systems and all possible cross-interactions. Activity area of each column's fitted curve is normalized by the maximum activity area of the promoter corresponding to that particular column (e.g., LLA/LLL or AAL/AAA). (B) The lux system demonstrates both signal and promoter crosstalk to the las system, while the las is orthogonal to the lux system. (C) The lux and rpa systems are signal orthogonal but demonstrate two-way promoter crosstalk. (D) The las and tra systems are promoter orthogonal but demonstrate two-way signal crosstalk. (E) The rpa and tra systems are completely orthogonal.

be used as a master control of certain systems, allowing for circuits to be triggered only by external input. In general, the EC_{50} is useful for predicting relative performances of a particular R-protein across ligands. However, it tells you nothing about the raw expression levels, so it is not the best metric as a standard of performance. For instance, RRR is the most sensitive of all constructs with an EC_{50} of 0.5 nM (Figure 4B) but only has a fold change of 28 (Figure 4A), meanwhile RLL is 3 orders of magnitude less sensitive (Figure 4B) yet has a fold change of nearly 65 (Figure 4A).

The hill slope provides information about how sensitive the R-protein is to its ligand and whether the binding appears cooperative. It is common to attribute digital, or near-digital, responses to QS circuits, but this is inconsistent with the reality of biological systems, as most canonical QS systems have hill slopes around 1 (Table S1). Nevertheless, synthetic biologists may still want to choose the most digital construct possible (RRR) when constructing their circuit, or possibly the most linear (RLT). To quantify and compare the performance of these various QS circuits, activity area was found to be the most useful characteristic. This is consistent with a recent study, which reported AUC to be a better comparison method than EC_{50} .⁶⁷ Activity area includes all aspects of the response curve; that is, less leakiness, greater fold change, higher sensitivity, and lower EC_{50} s all contribute to increasing the activity area (Figure 4C, Table S1), making it an especially informative performance standard.

Therefore, activity area was used to compare the performances of all of the different systems. As an example, the activity area of LuxR and Plux with an off-target HSL (LLT) was divided by the canonical response (LLL), and it was seen that 3OC8 activated LuxR at 96% of its max efficiency (Figure 5A). Similarly, the activity area of RpaR with pC-HSL and the Plux promoter (LRR) was normalized by the response of the canonical lux system (LLL), and it was observed that, at its best, RpaR activated the Plux promoter at 87% of the promoter's maximum observed output over the concentration range in this study (Figure 5A). This allows quick evaluation of general

properties of these components. For instance, the Plux and Prpa* promoters are promiscuous, while Plas and Ptra* are very specific to their particular R-protein. Unexpectedly, since the acyl-HSL's of lux, tra, and las are so similar (Figure S1), there is a large amount of signal crosstalk between their R-proteins. Conversely, since p-coumaroyl, an aryl-HSL, has a much different structure (Figure S1) than the others, it is recognizable by only RpaR, and RpaR cannot recognize the other signals.

The result of this multiplex assay offers insight into many unexpected pairings of receptor, ligand, and promoter that synthetic biologists can utilize for various circuit functions. Since the lux system is widely used, it is important to note that using RpaR with pC-HSL in conjunction with Plux gives an almost identical fold change and hill slope but with higher sensitivity and lower leakiness, making this hybrid system a desirable alternative to the canonical lux circuit. Similarly, LasR with 3OC12 driving transcription off the Prpa* promoter is almost half as leaky as the canonical las circuit, while still giving a large fold change and low sensitivity (Table S1). Furthermore, comparing the activity area of two QS systems was found to be a useful method to quickly identify crosstalk and orthogonality.

2.4. Toward Microbial Consortia. Individual constructs have intrinsic value, however, circuits were evaluated for potential use in multisystem consortia by grouping their cross-interactions (Figure 5). Although lux and las have been used in numerous circuits before, they do exhibit a significant amount of crosstalk. Specifically, LuxR can become active by binding the 3OC12 of las, and an activated LasR protein can activate the Plux promoter. However, the Plas promoter is completely orthogonal to the lux system (with the caveat that LasR can become somewhat active at 100 μ M 3OC6). Taken together the lux/las system exhibits one-way orthogonality (Figure 5B) in the physiologically relevant concentration range.

Interestingly, although the lux and the rpa systems exhibited promoter crosstalk, they were signal orthogonal: they could not bind each other's ligand. This crosstalk dynamic implies that they could function independently as long as their promoters

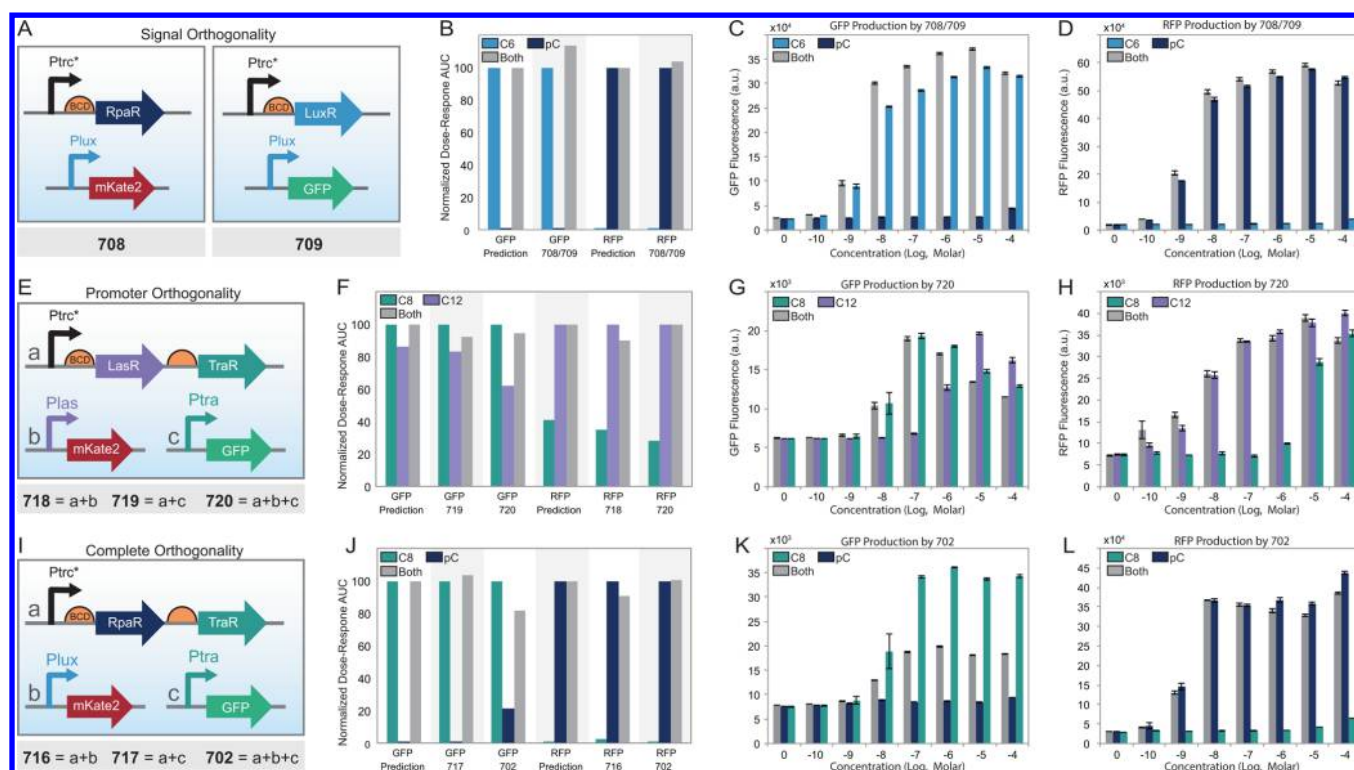


Figure 6. Verification of QS component orthogonality. (A) Genetic schematic of signal orthogonal strains 708 and 709. (B) A 1:1 coculture of 708 and 709 was subjected to the full range of HSLs, and the AUC of the dose–response was compared to predictions based on their original characterization in Figure 3 and Table S1. For all predictions, it was assumed the canonical HSL would give the maximum response, so it was assumed providing both HSLs would still give an AUC of 100. Each experiment is normalized by the canonical response, such that the AUC of the GFP dose–response to C6–HSL is set to 100, making the ratio between columns in a set the point of comparison. For example, the 708/709 GFP column set follows this formula: (AUC-C6/AUC-C6), (AUC-pC/AUC-C6), (AUC-Both/AUC-C6). (C, D) Raw fluorescence expression of the 708/709 coculture. Error bars represent SEM ($n = 4$). (E) Genetic schematic of promoter orthogonal strains 718, 719, and 720. (F) Normalized dose–response AUC showing similarity between predictions and *in vivo* results. (G, H) Raw fluorescence expression of 720. Raw expression of 718 and 719 is available in Figure S5. (I) Genetic schematic of complete orthogonal strains 716, 717, and 702. (J) Normalized dose–response AUC of predictions and *in vivo* results. (K, L) Raw fluorescence expression of 702. Raw expression of 716 and 717 is available in Figure S5. Error bars represent SEM ($n = 4$).

are physically compartmentalized (e.g., contained within different cell types, Figure 5C). Therefore, a coculture of lux-responsive and rpa-responsive cells could be orthogonally controlled by their diffusible signal into the 100 μ M concentration range. The las and rpa systems also exhibited signal orthogonality, with even less crosstalk at 100 μ M.

There were two system pairs that exhibited signal crosstalk but were promoter orthogonal: the lux/tra pair and the tra/las pair (Figure 5D). LuxR and LasR could not activate Ptr^a*, and TraR could not activate Plux or Plas; however, with such similar HSLs, either of the systems' ligand worked to activate both R-proteins to a significant degree. Although signal crosstalk with promoter orthogonality will not explicitly allow for differential control of specific strains, these systems could be used for OR-gates or competitive-inhibition-based circuits.⁶⁸

Additionally, the tra and rpa systems exhibited both signal and promoter orthogonality, characterizing them as completely orthogonal (Figure 5E). These systems would allow for the control of two quorum sensing systems not only in the same culture but within the same cell or compartment. Both R-proteins are incapable of binding to either the nonspecific promoter or the nonspecific ligand. While signal-orthogonality is sufficient for creating complex population dynamics, assuming each cell is controlled by one system, complete orthogonality can accomplish population dynamics as well as

more advanced internal signaling such as the maintenance of two asynchronous, noninterfering oscillators.

To validate the characterization of our constructs and verify their potential for synthetic ecologies, we tested these three communication modules in the same culture or cell (Figure 6 and Figure S5). Signal orthogonal strains (Figure 6A) were cocultured and exposed to 3OC6HSL (C6), pC, or both HSLs. Their dose–response profiles (Figure 6C–D) were used to generate AUC ratios which were compared to response predictions based on the individual constructs' previous characterization (Figure 6B). The same was done for promoter orthogonal strains (Figure 6E–H) and complete orthogonal strains (Figure 6I–L) with their respective HSLs.

In all cases, the components behaved very similarly to their predicted response, suggesting these components will translate well into applied circuits. It is important to note that the apparent cross-talk in the GFP-702 column (Figure 6J) is due to growth defects. The basal level of GFP remains the same (Figure 6K); however, the OD decreases with increased pC–HSL (Figure S6C) due to the heavy metabolic load of producing RFP and harboring three relatively high-copy plasmids. Since all fluorescence data are OD normalized, the subsequent AUC calculations misrepresent a decrease in OD as an increase in OD-normalized fluorescence. These growth defects are likely also responsible for the decrease in GFP

production under both HSLs (Figure 6K). The complete orthogonality of the rpa/tra systems is further confirmed by Strain 717 which would show the same GFP–AUC ratios as 702 if the cross-talk were real, but having normal growth under all conditions (Figure S6B), it more accurately demonstrates tra's unresponsiveness to pC-HSL and RpaR (Figure 6J and Figure SSE).

Lastly, to further the case for rpa's utility to synthetic biology, we recognize the importance of being able to produce pC-HSL *in vivo*. Preliminary data appears to show that the native sequence from *R. palustris* can be expressed in *E. coli* and activate the Rpa system (Figure S7). Further tests are needed to thoroughly prove its functionality, but our data suggest RpaI and the rpa components have potential to be used in future dynamical QS systems.

Characterizing the interactions of just four different quorum sensing systems resulted in the identification of many potential circuit components for use in a variety of synthetic biology applications. Our study demonstrates that because of the natural abundance of quorum sensing systems and their ease of engineering, due to protein and promoter modularity, QS is a very attractive tool for the development of next generation genetic circuits and the programming of microbial consortia.

Although completely orthogonal systems have straightforward use cases, we hypothesize that promoter-orthogonal and signal-orthogonal pairs offer their own unique advantages as certain levels of crosstalk may be desirable in creating more interesting circuits with complex dynamics. We anticipate that the unique crosstalk interactions and affinities of the different QS combinations characterized in this study can be used to this advantage. Furthermore, the possibilities unlocked by QS circuitry will only grow as more QS systems are characterized and created. Given the ease of promoter and protein engineering of QS components, it is clear that these systems could be further optimized by modifying either the ligand binding, DNA-binding, or sigma-factor-recruiting domains. As more novel QS systems are engineered, the various types and strengths of cross-interaction will be a very useful tool set for real-world applications in synthetic biology.

METHODS SUMMARY

Plasmids and Strains. The plasmids used in this study are described in Table S3. All studies were done in the “EK” *E. coli* DIAL strain provided by Josh Kittelson;⁶⁹ this strain is necessary for proper propagation of plasmids due to R6K and ColE2 origins of replication used in all plasmids. Promoters and UTRs described by Mutalik *et al.*^{70,71} were synthesized de novo from IDT. Genomes of *Rhodopseudomonas palustris* (RpaR), *Rhodobacter sphaeroides* (CerR), *Sinorhizobium meliloti* (SinR, ExpR), and *Serratia marcescens* (SmaR) were obtained from ATCC. Lux, las, and rhl were obtained in lab and tra was taken from iGEM pSB1C3-BBa-K916000 found in Distribution Plate 2, Well 9J.

Fluorescence Expression Measurements. Cells were prepared for plate reader experiments as follows: strains were grown overnight and then reseeded in a 1:1000 dilution into fresh media containing ampicillin and spectinomycin resistance. The dilution was allowed to grow for about 4 h until it reached OD \approx 0.1. Then, the cell culture were distributed into a 96-well plate (180 μ l final volume per well) and induced with a range of AHL concentrations (1:10 serial dilutions were done from 1×10^{-4} M to 1×10^{-10} M or 1×10^{-14} M). AHLs stocks were dissolved in DMSO, resulting in a max DMSO concentration of

1% in LB. After induction, the cells were allowed to grow for 3 h until OD \approx 0.5 at which point they were measured with a Tecan infinite M200Pro for OD600 as well as GFP fluorescence with the following fixed settings: no top, fixed gain of 61, excitation of 485 nm, emission of 520 nm, and Z-position of 19500. All GFP measurements were normalized by dividing their raw values by the OD of that well to give a “per-cell” measurement and account for slight differences in growth rates. For Figure 6, the same methods were used, except gain regulation was used to find an optimal gain for each individual experiment, and RFP levels were measured with an excitation of 580 nm and an emission of 620 nm.

Dose–Response Fitting. A Matlab script utilizing non-linear regression was used to fit the plate reader measurements to the described dose–response equation. The script by Ritchie Smith was obtained here via mathworks.com and was slightly modified for this study. The script takes the dose and response matrices as inputs, fits the curve, and outputs the min, max, Hill coefficient, EC50, and AUC of the curve.

ASSOCIATED CONTENT

Supporting Information

The Supporting Information is available free of charge on the ACS Publications website at DOI: [10.1021/acssynbio.5b00286](https://doi.org/10.1021/acssynbio.5b00286).

Excel file with raw data and dose–response curves (XLSX)

Supplementary figures and tables including promoter sequences and plasmids used for all experiments (PDF)

AUTHOR INFORMATION

Corresponding Author

*E-mail: hasty@ucsd.edu. Tel.: 858 822 3442.

Notes

The authors declare no competing financial interest.

ACKNOWLEDGMENTS

This material is based upon work supported by the National Science Foundation Graduate Research Fellowship under Grant No. DGE-1144086. Any opinion, findings, and conclusions or recommendations expressed in this material are those of the authors(s) and do not necessarily reflect the views of the National Science Foundation. National Institutes of Health and General Medicine (R01GM69811).

REFERENCES

- (1) Khalil, A. S., and Collins, J. J. (2010) Synthetic biology: applications come of age. *Nat. Rev. Genet.* 11, 367–379.
- (2) Ro, D.-K., Paradise, E. M., Ouellet, M., Fisher, K. J., Newman, K. L., Ndungu, J. M., Ho, K. A., Eachus, R. A., Ham, T. S., Kirby, J., and Keasling, J. D. (2006) Production of the antimalarial drug precursor artemisinic acid in engineered yeast. *Nature* 440, 940–943.
- (3) McDaniel, R., and Weiss, R. (2005) Advances in synthetic biology: on the path from prototypes to applications. *Curr. Opin. Biotechnol.* 16, 476–483.
- (4) Dueber, J. E., Wu, G. C., Malmirchegini, G. R., Moon, T. S., Petzold, C. J., Ullal, A. V., Prather, K. L., and Keasling, J. D. (2009) Synthetic protein scaffolds provide modular control over metabolic flux. *Nat. Biotechnol.* 27, 753–759.
- (5) Kizer, L., Pitera, D. J., Pfleger, B. F., and Keasling, J. D. (2008) Application of functional genomics to pathway optimization for increased isoprenoid production. *Applied and environmental microbiology* 74, 3229–3241.

- (6) Zhu, M. M., Lawman, P. D., and Cameron, D. C. (2002) Improving 1, 3-Propanediol Production from Glycerol in a Metabolically Engineered *Escherichia coli* by Reducing Accumulation of sn-Glycerol-3-phosphate. *Biotechnology progress* 18, 694–699.
- (7) Barbirato, F., Grivet, J. P., Soucaille, P., and Bories, A. (1996) 3-Hydroxypropionaldehyde, an inhibitory metabolite of glycerol fermentation to 1, 3-propanediol by enterobacterial species. *Appl. Environ. Microbiol.* 62, 1448–1451.
- (8) Brenner, K., and Arnold, F. H. (2011) Self-organization, layered structure, and aggregation enhance persistence of a synthetic biofilm consortium. *PLoS One* 6, e16791–e16791.
- (9) Carlson, R. P., and Taffs, R. L. (2010) Molecular-level tradeoffs and metabolic adaptation to simultaneous stressors. *Curr. Opin. Biotechnol.* 21, 670–676.
- (10) Kneitel, J. M., and Chase, J. M. (2004) Trade-offs in community ecology: linking spatial scales and species coexistence. *Ecology Letters* 7, 69–80.
- (11) McMahon, K. D., Martin, H. G., and Hugenholtz, P. (2007) Integrating ecology into biotechnology. *Curr. Opin. Biotechnol.* 18, 287–292.
- (12) Brenner, K., You, L., and Arnold, F. H. (2008) Engineering microbial consortia: a new frontier in synthetic biology. *Trends Biotechnol.* 26, 483–489.
- (13) Pandhal, J., and Noirel, J. (2014) Synthetic microbial ecosystems for biotechnology. *Biotechnol. Lett.* 36, 1141–1151.
- (14) De Roy, K., Marzorati, M., Van den Abbeele, P., Van de Wiele, T., and Boon, N. (2014) Synthetic microbial ecosystems: an exciting tool to understand and apply microbial communities. *Environ. Microbiol.* 16, 1472–1481.
- (15) Dunham, M. J. (2007) Synthetic ecology: a model system for cooperation. *Proc. Natl. Acad. Sci. U. S. A.* 104, 1741–1742.
- (16) Mee, M. T., Collins, J. J., Church, G. M., and Wang, H. H. (2014) Syntrophic exchange in synthetic microbial communities. *Proc. Natl. Acad. Sci. U. S. A.* 111, E2149–E2156.
- (17) Arai, T., Matsuoka, S., Cho, H.-Y., Yukawa, H., Inui, M., Wong, S.-L., and Doi, R. H. (2007) Synthesis of *Clostridium cellulovorans* minicellulosomes by intercellular complementation. *Proc. Natl. Acad. Sci. U. S. A.* 104, 1456–1460.
- (18) Vinuselvi, P., and Lee, S. K. (2012) Engineered *Escherichia coli* capable of co-utilization of cellobiose and xylose. *Enzyme Microb. Technol.* 50, 1–4.
- (19) Bernstein, H. C., Paulson, S. D., and Carlson, R. P. (2012) Synthetic *Escherichia coli* consortia engineered for syntrophy demonstrate enhanced biomass productivity. *J. Biotechnol.* 157, 159–166.
- (20) Minty, J. J., Singer, M. E., Scholz, S. A., Bae, C.-H., Ahn, J.-H., Foster, C. E., Liao, J. C., and Lin, X. N. (2013) Design and characterization of synthetic fungal-bacterial consortia for direct production of isobutanol from cellulosic biomass. *Proc. Natl. Acad. Sci. U. S. A.* 110, 14592–14597.
- (21) Eiteman, M. A., Lee, S. A., and Altman, E. (2008) A co-fermentation strategy to consume sugar mixtures effectively. *J. Biol. Eng.* 2, 3.
- (22) Burmolle, M., Webb, J. S., Rao, D., Hansen, L. H., Sorensen, S. J., and Kjelleberg, S. (2006) Enhanced biofilm formation and increased resistance to antimicrobial agents and bacterial invasion are caused by synergistic interactions in multispecies biofilms. *Applied and environmental microbiology* 72, 3916–3923.
- (23) LaPara, T., Zakharova, T., Nakatsu, C., and Konopka, A. (2002) Functional and structural adaptations of bacterial communities growing on particulate substrates under stringent nutrient limitation. *Microb. Ecol.* 44, 317–326.
- (24) Fay, P. (1992) Oxygen relations of nitrogen fixation in cyanobacteria. *Microbiological reviews* 56, 340.
- (25) Shou, W., Ram, S., and Vilar, J. M. (2007) Synthetic cooperation in engineered yeast populations. *Proc. Natl. Acad. Sci. U. S. A.* 104, 1877–1882.
- (26) Balagaddé, F. K., Song, H., Ozaki, J., Collins, C. H., Barnet, M., Arnold, F. H., Quake, S. R., and You, L. (2008) A synthetic *Escherichia coli* predator-prey ecosystem. *Mol. Syst. Biol.* 4, 187.
- (27) West, S. A., Griffin, A. S., Gardner, A., and Diggle, S. P. (2006) Social evolution theory for microorganisms. *Nat. Rev. Microbiol.* 4, 597–607.
- (28) Ng, W.-L., and Bassler, B. L. (2009) Bacterial quorum-sensing network architectures. *Annu. Rev. Genet.* 43, 197.
- (29) Waters, C. M., and Bassler, B. L. (2005) Quorum sensing: cell-to-cell communication in bacteria. *Annu. Rev. Cell Dev. Biol.* 21, 319–346.
- (30) Miller, M. B., and Bassler, B. L. (2001) Quorum sensing in bacteria. *Annu. Rev. Microbiol.* 55, 165–199.
- (31) Davis, R. M., Muller, R. Y., and Haynes, K. A. (2015) Can the natural diversity of quorum-sensing advance synthetic biology. *Front. Bioeng. Biotechnol.* 3, No. fbioe.2015.00099, DOI: 10.3389/fbioe.2015.00099.
- (32) Hong, S. H., Hegde, M., Kim, J., Wang, X., Jayaraman, A., and Wood, T. K. (2012) Synthetic quorum-sensing circuit to control consortial biofilm formation and dispersal in a microfluidic device. *Nat. Commun.* 3, 613.
- (33) Kobayashi, H., Kærn, M., Araki, M., Chung, K., Gardner, T. S., Cantor, C. R., and Collins, J. J. (2004) Programmable cells: interfacing natural and engineered gene networks. *Proc. Natl. Acad. Sci. U. S. A.* 101, 8414–8419.
- (34) Prindle, A., Selimkhanov, J., Li, H., Razinkov, I., Tsimring, L. S., and Hasty, J. (2014) Rapid and tunable post-translational coupling of genetic circuits. *Nature* 508, 387–391.
- (35) Danino, T., Mondragón-Palomino, O., Tsimring, L., and Hasty, J. (2010) A synchronized quorum of genetic clocks. *Nature* 463, 326–330.
- (36) Basu, S., Gerchman, Y., Collins, C. H., Arnold, F. H., and Weiss, R. (2005) A synthetic multicellular system for programmed pattern formation. *Nature* 434, 1130–1134.
- (37) Payne, S., Li, B., Cao, Y., Schaeffer, D., Ryser, M. D., and You, L. (2013) Temporal control of self-organized pattern formation without morphogen gradients in bacteria. *Mol. Syst. Biol.* 9, 697.
- (38) Saeidi, N., Wong, C. K., Lo, T.-M., Nguyen, H. X., Ling, H., Leong, S. S. J., Poh, C. L., and Chang, M. W. (2011) Engineering microbes to sense and eradicate *Pseudomonas aeruginosa*, a human pathogen. *Mol. Syst. Biol.* 7, 521.
- (39) Brenner, K., Karig, D. K., Weiss, R., and Arnold, F. H. (2007) Engineered bidirectional communication mediates a consensus in a microbial biofilm consortium. *Proc. Natl. Acad. Sci. U. S. A.* 104, 17300–17304.
- (40) Brockman, I. M., and Prather, K. L. (2015) Dynamic metabolic engineering: New strategies for developing responsive cell factories. *Biotechnol. J.* 10, 1360.
- (41) Srimani, J. K., and You, L. (2014) Emergent Dynamics from Quorum Eavesdropping. *Chem. Biol.* 21, 1601–1602.
- (42) Pai, A., Tanouchi, Y., and You, L. (2012) Optimality and robustness in quorum sensing (QS)-mediated regulation of a costly public good enzyme. *Proc. Natl. Acad. Sci. U. S. A.* 109, 19810–19815.
- (43) Tsao, C.-Y., Hooshangi, S., Wu, H.-C., Valdes, J. J., and Bentley, W. E. (2010) Autonomous induction of recombinant proteins by minimally rewiring native quorum sensing regulon of *E. coli*. *Metab. Eng.* 12, 291–297.
- (44) Wu, F., Menn, D. J., and Wang, X. (2014) Quorum-Sensing Crosstalk-Driven Synthetic Circuits: From Unimodality to Trimodality. *Chem. Biol.* 21, 1629–1638.
- (45) Zhu, J., and Winans, S. C. (1999) Autoinducer binding by the quorum-sensing regulator TraR increases affinity for target promoters in vitro and decreases TraR turnover rates in whole cells. *Proc. Natl. Acad. Sci. U. S. A.* 96, 4832–4837.
- (46) Fuqua, C., and Winans, S. C. (1996) Conserved cis-acting promoter elements are required for density-dependent transcription of *Agrobacterium tumefaciens* conjugal transfer genes. *J. Bacteriol.* 178, 435–440.

- (47) White, C. E., and Winans, S. C. (2007) The quorum-sensing transcription factor TraR decodes its DNA binding site by direct contacts with DNA bases and by detection of DNA flexibility. *Mol. Microbiol.* 64, 245–256.
- (48) Brophy, J. A., and Voigt, C. A. (2014) Principles of genetic circuit design. *Nat. Methods* 11, 508–520.
- (49) Chuang, J. S. (2012) Engineering multicellular traits in synthetic microbial populations. *Curr. Opin. Chem. Biol.* 16, 370–378.
- (50) Marchand, N., and Collins, C. H. (2013) Peptide-based communication system enables *Escherichia coli* to *Bacillus megaterium* interspecies signaling. *Biotechnol. Bioeng.* 110, 3003–3012.
- (51) Quan, D. N., Tsao, C.-Y., Wu, H.-C., and Bentley, W. E. (2016) Quorum Sensing Desynchronization Leads to Bimodality and Patterned Behaviors. *PLoS Comput. Biol.* 12, e1004781.
- (52) Shong, J., and Collins, C. H. (2013) Engineering the *esaR* promoter for tunable quorum sensing-dependent gene expression. *ACS Synth. Biol.* 2, 568–575.
- (53) Gray, K. M., and Garey, J. R. (2001) The evolution of bacterial LuxI and LuxR quorum sensing regulators. *Microbiology* 147, 2379–2387.
- (54) Fuqua, C., Winans, S. C., and Greenberg, E. P. (1996) Census and consensus in bacterial ecosystems: the LuxR-LuxI family of quorum-sensing transcriptional regulators. *Annu. Rev. Microbiol.* 50, 727–751.
- (55) Schaefer, A. L., Greenberg, E., Oliver, C. M., Oda, Y., Huang, J. J., Bittan-Banin, G., Peres, C. M., Schmidt, S., Juhaszova, K., and Sufirin, J. R. (2008) A new class of homoserine lactone quorum-sensing signals. *Nature* 454, 595–599.
- (56) Hirakawa, H., Oda, Y., Phattarasukol, S., Armour, C. D., Castle, J. C., Raymond, C. K., Lappala, C. R., Schaefer, A. L., Harwood, C. S., and Greenberg, E. P. (2011) Activity of the *Rhodopseudomonas palustris* p-coumaroyl-homoserine lactone-responsive transcription factor RpaR. *Journal of bacteriology* 193, 2598–2607.
- (57) Swift, S., Karlyshev, A. V., Fish, L., Durant, E. L., Winson, M. K., Chhabra, S. R., Williams, P., Macintyre, S., and Stewart, G. (1997) Quorum sensing in *Aeromonas hydrophila* and *Aeromonas salmonicida*: identification of the LuxRI homologs AhyRI and AsaRI and their cognate N-acylhomoserine lactone signal molecules. *Journal of bacteriology* 179, 5271–5281.
- (58) Thomson, N., Crow, M., McGowan, S., Cox, A., and Salmond, G. (2000) Biosynthesis of carbapenem antibiotic and prodigiosin pigment in *Serratia* is under quorum sensing control. *Mol. Microbiol.* 36, 539–556.
- (59) Puskas, A., Greenberg, E. á., Kaplan, S., and Schaefer, A. á. (1997) A quorum-sensing system in the free-living photosynthetic bacterium *Rhodobacter sphaeroides*. *Journal of bacteriology* 179, 7530–7537.
- (60) Charoenpanich, P., Meyer, S., Becker, A., and McIntosh, M. (2013) Temporal expression program of quorum sensing-based transcription regulation in *Sinorhizobium meliloti*. *Journal of bacteriology* 195, 3224–3236.
- (61) Garde, C., Bjarnsholt, T., Givskov, M., Jakobsen, T. H., Hentzer, M., Claussen, A., Sneppen, K., Ferkinghoff-Borg, J., and Sams, T. (2010) Quorum sensing regulation in *Aeromonas hydrophila*. *J. Mol. Biol.* 396, 849–857.
- (62) Slater, H., Crow, M., Everson, L., and Salmond, G. P. (2003) Phosphate availability regulates biosynthesis of two antibiotics, prodigiosin and carbapenem, in *Serratia* via both quorum-sensing-dependent and-independent pathways. *Mol. Microbiol.* 47, 303–320.
- (63) Karig, D., and Weiss, R. (2005) Signal-amplifying genetic circuit enables in vivo observation of weak promoter activation in the Rhl quorum sensing system. *Biotechnol. Bioeng.* 89, 709–718.
- (64) Vannini, A., Volpari, C., Gargioli, C., Muraglia, E., Cortese, R., De Francesco, R., Neddermann, P., and Di Marco, S. (2002) The crystal structure of the quorum sensing protein TraR bound to its autoinducer and target DNA. *EMBO journal* 21, 4393–4401.
- (65) Fuqua, C., and Greenberg, E. P. (2002) Listening in on bacteria: acyl-homoserine lactone signalling. *Nat. Rev. Mol. Cell Biol.* 3, 685–695.
- (66) Yadav, B., Pemovska, T., Szwajda, A., Kuleskiy, E., Kontro, M., Karjalainen, R., Majumder, M. M., Malani, D., Murumägi, A., and Knowles, J. (2014) Quantitative scoring of differential drug sensitivity for individually optimized anticancer therapies. *Sci. Rep.* 4, No. srep05193, DOI: 10.1038/srep05193.
- (67) Huang, S., and Pang, L. (2012) Comparing statistical methods for quantifying drug sensitivity based on in vitro dose-response assays. *Assay Drug Dev. Technol.* 10, 88–96.
- (68) Chickarmane, V., Kholodenko, B. N., and Sauro, H. M. (2007) Oscillatory dynamics arising from competitive inhibition and multisite phosphorylation. *J. Theor. Biol.* 244, 68–76.
- (69) Kittleson, J. T., Cheung, S., and Anderson, J. C. (2011) Rapid optimization of gene dosage in *E. coli* using DIAL strains. *J. Biol. Eng.* 5, 10.
- (70) Mutalik, V. K., Guimaraes, J. C., Cambray, G., Lam, C., Christoffersen, M. J., Mai, Q.-A., Tran, A. B., Paull, M., Keasling, J. D., Arkin, A. P., and Endy, D. (2013) Precise and reliable gene expression via standard transcription and translation initiation elements. *Nat. Methods* 10, 354–360.
- (71) Mutalik, V. K., Guimaraes, J. C., Cambray, G., Mai, Q.-A., Christoffersen, M. J., Martin, L., Yu, A., Lam, C., Rodriguez, C., and Bennett, G. (2013) Quantitative estimation of activity and quality for collections of functional genetic elements. *Nat. Methods* 10, 347–353.